Estimability for robot localization in a structured environment with outliers

Clara Gondot
CLEO-CMA
Bagnols-sur-Cèze, France
cgt@cleo-cma.com

Fabrice Le Bars
Lab-STICC, ENSTA
Brest, France
fabrice.le_bars@ensta.fr

Luc Jaulin
Lab-STICC, ENSTA
Brest, France
luc.jaulin@ensta.fr

***Abstract*—Confidence in sensor measurements is essential for the localization of autonomous robots. But in critical contexts, when encountering sensor failures, we still need to know how our algorithms will behave. In this article, interval analysis and set-based inversion techniques are used to handle measurement outliers and bounded uncertainties in both sensor data and environmental knowledge. We are ultimately able to guarantee estimation performance without advanced statistical models or complex and numerous simulations.**

The main result is a computation method of a guaranteed estimability in a context with outliers and uncertain environmental parameters by leveraging a relaxed intersection approach. This process is illustrated in a simple experiment of the static localization of a telemeter-equipped robot in a 2-D structured environment. A simulated environment is used to generate estimability maps, allowing to visualize localization performance before deployment, providing a practical tool for mission planning and system monitoring.

***Index Terms*—Planning and Navigation; Mobile Robots; Identification and Estimation in Mechatronics**

I. Introduction

Autonomous vehicles operating in sensitive and structured industrial environments, such as maintenance facilities, decommissioning sites, or underground mining sites, must reliably localize themselves to execute critical missions. Many of these environments are inherently hazardous for human operators, making robust automated systems essentials.

In known environments, localization uses prior information paired with sensor measurements to estimate the system's position. However, real missions and critical applications may involve sensor failure, outliers in measurements, or uncertainties in the environment model. Even in such contexts, it is crucial to provide guarantees on the performances of the position estimation, as well as to understand the effect of such failures and uncertainties on the localization results.

Conventional probabilistic methods [1] can be used to define a localizability metric. Several metrics have been proposed in the literature. Walther et al. [2] simulate point clouds and use a Monte-Carlo particle filter, feeding a binary localizability accuracy metric to a neural network. Roy and Thrun [3] use Markov localization and the associated probability distribution over the state space, scored with an entropy function, high when the distribution is spread, low when the results are accurate. Zhen et al. [4] model the observations as a linear system, and process the constraint matrix until a SVD associating eigenvalues to a reduced number of constraints — lower eigenvalues means lower solvability of the system. However, these metrics are usually tied to specific estimation models and prior assumptions on error distributions, which makes them difficult to compare across applications and less suited to situations with outliers or poorly known error statistics. In contrast, interval analysis [5] and set-based methods handle bounded uncertainties and outliers in a guaranteed way, without requiring an extensive probabilistic model of the errors. Set-based methods allowed us to define a theoretically universal method of estimability for a constrained system.

This article focuses on interval based computation of estimability [6]. While previous works took into account a potential bounded noise on measurements, in this article we broaden the guaranteed estimability definition in the presence of outliers and external parameters. This definition is then applied to the localization of a robot equipped with range sensors in a structured environment.

Section II of this article dives into interval analysis concepts and tools, to ultimately define the estimability computation. In Section III, these concepts are applied to the localization of a vehicle in a known planar environment described by segments. Lastly, results and potential perspectives are discussed in Section IV before concluding.

II. Theory

A. Interval Analysis introduction

In this article, unknown values are represented as intervals of $\mathbb{R}$ for the one-dimensional case, vectors of intervals or boxes for the multi-dimensional case in $\mathbb{R}^n$. We will respectively denote $\mathbb{IR}$ and $\mathbb{IR}^n$ the sets of intervals and boxes.

Let us note $x \in \mathbb{R}$. The interval representation of x will be noted $[x] \in \mathbb{IR}$. If $[x] = [x^-, x^+]$, $(x^-, x^+) \in \mathbb{R}^2$, then the width of $[x]$ is the difference $\text{width}([x]) = x^+ - x^-$. Vectors, as well as their interval representation, will be noted in bold, e.g. $\mathbf{x} = (x_1 \dots x_n)^T \in \mathbb{R}^n$ and $[\mathbf{x}] = [x_1] \times \cdots \times [x_n] \in \mathbb{IR}^n$. Lastly, when given a function $\mathbf{f} : \mathbb{R}^n \to \mathbb{R}^m$, then $[\mathbf{f}] : \mathbb{IR}^n \to \mathbb{IR}^m$ is an inclusion function [7], which must satisfy:

$$\forall [\mathbf{a}] \in \mathbb{IR}^n, \mathbf{f}([\mathbf{a}]) \subseteq [\mathbf{f}]([\mathbf{a}]) \tag{1}$$

Interval analysis defines a set of mathematical tools that allows to process these intervals, and to apply usual operations — i.e. intersection, union, arithmetic operations, usual functions —

in a way that is guaranteed to be sound. Interval analysis has been used successfully on many problems such as SLAM [8], [9] or visual processing [10].

B. Set Contraction

In some problems, direct computation over interval sets is intractable, and we require processes that propagate constraints while containing the result. This is done via set contraction, which is the process of applying constraints to reduce the width of an interval. The result of a contraction is an interval that is included in the original one (*contractance*), and that is guaranteed to contain all the possible values of the variable given the constraints applied (*consistency*) [7].

When solving a Constraint Satisfaction Problem (CSP), which takes into account several constraints and intervals variables, the contraction algorithm is applied iteratively, until there is no more reduction of the input intervals.

C. Set inversion

The estimation algorithm's goal is to approximate an unknown vector $\mathbf{p}$, using a large set of parameters $\mathbf{w}$, and multiple measurements $(y_i)_{1\leq i\leq n}$. These quantities are linked through the observation functions:

$$\forall i \in [\![1,n]\!], f_i : \begin{array}{l} \mathbb{R}^l \times \mathbb{R}^m \to \mathbb{R} \\ (\mathbf{p},\mathbf{w}) \mapsto y_i \end{array} \tag{2}$$

It is assumed that the error on the measurements is bounded. If we know a starting estimate $[\mathbf{p}] \in \mathbb{IR}^l$, the bounded interval vector of possible parameters $[\mathbf{w}] \in \mathbb{IR}^m$ and $[y_i] \in \mathbb{IR}$ the intervals containing each measurement, then the estimation problem aims to find:

$$\mathbb{P} = \{\mathbf{p} \in [\mathbf{p}] | \exists \mathbf{w} \in [\mathbf{w}], \forall i \in [\![1,n]\!], f_i(\mathbf{p},\mathbf{w}) \in [y_i]\} \tag{3}$$

This implies:

$$\mathbb{P} \subseteq \begin{array}{r} \{\mathbf{p} \in [\mathbf{p}] | \exists \mathbf{w}_1 \in [\mathbf{w}], f_1(\mathbf{p},\mathbf{w}_1) \in [y_1], \dots, \\ \exists \mathbf{w}_n \in [\mathbf{w}], f_n(\mathbf{p},\mathbf{w}_n) \in [y_n]\} \end{array} \tag{4}$$

$$\Leftrightarrow \mathbb{P} \subseteq \bigcap_{i=1}^{n} \{\mathbf{p} \in [\mathbf{p}] | \exists \mathbf{w} \in [\mathbf{w}], f_i(\mathbf{p},\mathbf{w}) \in [y_i]\} \tag{5}$$

$$\Rightarrow \mathbb{P} \subseteq \bigcap_{i=1}^{n} \{\mathbf{p} \in [\mathbf{p}] | \exists \mathbf{w} \in [\mathbf{w}], [f_i](\mathbf{p},\mathbf{w}) \in [y_i]\} \tag{6}$$

The process of estimating $\mathbb{P}$ is the inversion of the set of known measurements [7], which is illustrated in Figure 1. This inversion via intersection process is valid as long as all the measurements are within the tolerated error. The following concept shows a way to account for potential outliers among the measurements.

D. Relaxed intersection

A first enhancement to the set inversion is to make it robust to outliers in measurements. We make the following assumption:

MNO (Maximal Number of Outliers) assumption: Outliers measurements may exist, but their number never exceeds a maximum of q.

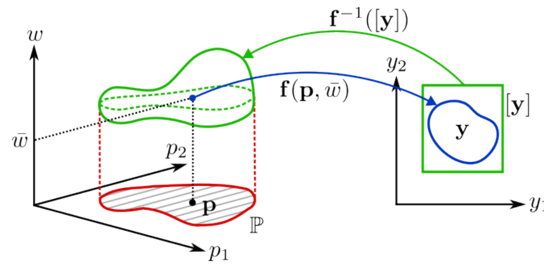

Fig. 1: Illustration of the set-inversion problem with a single measurement $\mathbf{y}$ and 1-dimensional parameter w. The unknown pair $(\mathbf{p}, \bar{w})$ generates a measurement $\mathbf{y}$ in blue. The goal is to estimate $\mathbb{P} = \mathbf{f}^{-1}([\mathbf{y}])$ in the red crossed out area.

In Figure 2, the relaxed intersection of sets, i.e. the intersetion with outliers is illustrated. Let us consider n sets. The q-relaxed intersection contains points which belong to at least $n-q$ sets. Thus, up to q of the sets can *disagree* with the final result. This process does not determine which ones are the outliers — perspective on outlier identification are discussed in Section IV.

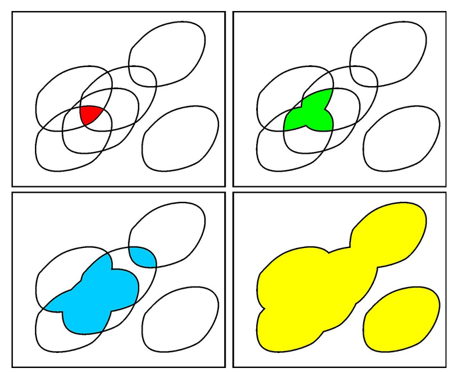

Fig. 2: Illustration of the q-relaxed intersection with $n = 6$ disagreeing sets, and $q \in \{2, 3, 4, 5\}$ (from top-left to bottom-right) [11].

Let us name $[\mathbf{p}_i]$ an interval vector such that $\{\mathbf{p} \in [\mathbf{p}] | \exists \mathbf{w}_i \in [\mathbf{w}], [f_i](\mathbf{p},\mathbf{w}_i) \in [y_i]\} \subseteq [\mathbf{p}_i]$. The result parameter estimation is now the *relaxed* intersection of said $[\mathbf{p}_i]$ boxes:

$$\mathbb{P} \subseteq \bigcap_{i \in [\![1,n]\!]}^{\{q\}} [\mathbf{p}_i] \tag{7}$$

Relaxed intersections have been used for other localization algorithms, with a temporal evolution function [12].

E. RSIVIA Algorithm

A major setback for the set-inversion is to have to start with a very wide starting vector of intervals. Let $[\mathbf{x}] \in \mathbb{IR}^n$ be this vector. To reduce its width, we bisect it, often along its largest dimension, to get two sub-boxes. The Relaxed Set Inverter Via Interval Analysis (RSIVIA) [12] is used. The RSIVIA algorithm uses the following principle: after using the set-inversion algorithm described before, if the result is not empty, bisect the result and restart the algorithm with the two smaller boxes. This allows to repeat the inversion process on smaller and smaller boxes, until a stopping condition is met. This condition can be on the number of iterations, or on the size of the boxes considered. In the simple version used here, when the stopping condition is met, the result is added to a list of solution sets.

F. Estimability

We described a method to interpret measurements and estimate $\mathbf{p}$. The next addition of this article is the use of a guaranteed tool to estimate the performances of said method. As described in [6], the first step is to find the other vectors that can yield the same measurements as $\mathbf{p}$, here with any environmental parameter $\mathbf{w}$. The hypothesis was made that there is a bounded noise $e \in E_i, E_i \subset \mathbb{R}$ on each measurement, such that:

$$y_i = f_i(\mathbf{p}, \mathbf{w}) + e \tag{8}$$

The goal is to compute the other vectors $\hat{\mathbf{p}}$ which are estimable from the measurements $(y_i)_{1 \le i \le n}$, i.e. vectors which satisfy:

$$\begin{aligned} &\exists(\mathbf{w}, \mathbf{w}') \in [\mathbf{w}]^2, \forall i, \exists(e_1, e_2) \in E_i^2, \\ &\qquad f_i(\hat{\mathbf{p}}, \mathbf{w}') + e_1 = f_i(\mathbf{p}, \mathbf{w}) + e_2 \end{aligned} \tag{9}$$

From this, let us define the i-th potential observation set, for any environmental parameter:

$$\mathbb{Y}_i(\mathbf{p}) = \{f_i(\mathbf{p}, \mathbf{w}) + e_2 - e_1 \mid \mathbf{w} \in [\mathbf{w}], (e_1, e_2) \in E_i^2\} \tag{10}$$

The vectors estimable from $\mathbf{p}$ would then be:

$$\begin{aligned} \hat{\mathbb{P}}(\mathbf{p}) &= \{\hat{\mathbf{p}} \in [\hat{\mathbf{p}}] \mid \exists \mathbf{w} \in [\mathbf{w}], \forall i, f_i(\hat{\mathbf{p}}, \mathbf{w}) \in \mathbb{Y}_i(\mathbf{p})\} && (11) \\ &\subseteq \{\hat{\mathbf{p}} \in [\hat{\mathbf{p}}] \mid \forall i, \exists \mathbf{w} \in [\mathbf{w}], f_i(\hat{\mathbf{p}}, \mathbf{w}) \in \mathbb{Y}_i(\mathbf{p})\} && (12) \end{aligned}$$

In practice, the vector $\mathbf{p}$ is unknown, and is estimated via a known algorithm through noisy observations. For any outlier, we have: $\mathbb{P} \subseteq \hat{\mathbb{P}}(\mathbf{p})$. In $\hat{\mathbb{P}}(\mathbf{p})$ are stored vectors that can be estimated from $\mathbf{p}$, hence its name: estimability set.

Next, let us take into account the MNO hypothesis. For two vectors $(\mathbf{p}, \hat{\mathbf{p}})$, we assume the presence of up-to q outliers among measurements. We need to find $n - q$ measurements compatible with $\mathbf{p}$, and $n - q$ other measurements compatible with $\hat{\mathbf{p}}$. Hence, there is a minimum of $n - 2 \cdot q$ common components between the two measurements vectors. Which ultimately translates to:

$$\hat{\mathbb{P}}(\mathbf{p}) \subseteq \bigcap_{1 \le i \le n}^{\{2 \cdot q\}} \{\hat{\mathbf{p}} \in [\hat{\mathbf{p}}] \mid \exists \mathbf{w} \in [\mathbf{w}], f_i(\hat{\mathbf{p}}, \mathbf{w}) \in \mathbb{Y}_i(\mathbf{p})\} \tag{13}$$

This estimability set includes any combination of outliers in the measurements and taken into account by the estimation process. $\hat{\mathbb{P}}(\mathbf{p})$ is computed through a set-inversion process alike the one described previously.

Once the approximation of $\hat{\mathbb{P}}(\mathbf{p})$ is computed, a metric is used to describe its size, and quantify the estimability of $\mathbf{p}$. This function must be monotonic and resulting in $\mathbb{R}^+$ [6]. For example, if the estimation process leaves us with a list of interval vectors as a result, this metric can be the width of the largest interval from the list or the sum or product of their width, the volume of their union etc. This metric is then used to map the performances of the estimation on the whole application domain. In the following section, the estimability set is illustrated for a localization problem.

III. Application

A. System and environment description

We consider the problem of the global static localization of a robot in a known planar environment. Let $[\mathbf{D}] \subset \mathbb{R}^2$ be the box containing the entire known environment, and $[\mathbf{p}]$ the box containing the estimation of the robot position. The heading of the robot is supposed to be contained in the interval $[\theta]$. Known structures are approximated by a list of m segments, named $(\mathbf{w}_k)_{1 \le k \le m}$. Let $([\mathbf{w}_k])_{1 \le k \le m} \subset \mathbb{IR}^{2 \cdot m}$ be the list of the known boxes containing said segments. The robot is equiped with a LiDAR, which emits n range measurements. Each measurement yields the distance $\tilde{d}_i$ from the position of the LiDAR to the nearest obstacle, with a direction $\tilde{\alpha}_i$, relative to the robot's heading. The maximum range of the LiDAR is $\overline{d}$. The error on the LiDAR measurements is bounded, and reflected in the two terms Δd and $\Delta \alpha$, such that the intervals used when processing a measurement $(\tilde{d}_i, \tilde{\alpha}_i)$ are:

$$[d_i] = [\tilde{d}_i - \Delta d/2, \tilde{d}_i + \Delta d/2] \tag{14}$$

$$[\alpha_i] = [\tilde{\alpha}_i - \Delta \alpha/2, \tilde{\alpha}_i + \Delta \alpha/2] \tag{15}$$

The i-th measurement is $[\mathbf{y}_i] = ([d_i], [\alpha_i])^T$. See Figure 3 for an illustration of the considered problem, with 5 known walls and their bounding boxes. The green outline represents the 4 range sensors measurements, accounting for the uncertainty on distance and orientation.

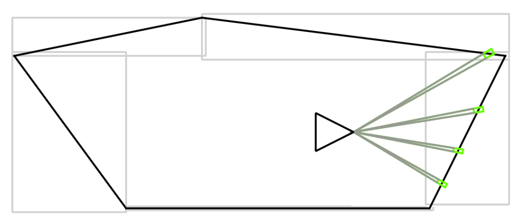

Fig. 3: Simulation of the system in a simple convex environment.

B. Localization Process

For each received measurement, the box $[\mathbf{p}]$ is translated along the rays defined by the measurement's direction and distance, in a manner similar to [9]. The translated box is contracted around the walls' boxes found in its area; then the reverse translation is applied. The Figure 4 illustrates this process for a single measurement. This is repeated for the n measurements, of which we take the q-relaxed intersection to obtain $[\mathbf{p}]$. The detailed operations used to compute $[\mathbf{p}]$ are given in the Procedure 1 below. For each measurement, we check in Line 3 if the measured distance is in the sensor range, otherwise the distance is changed to account for out of range

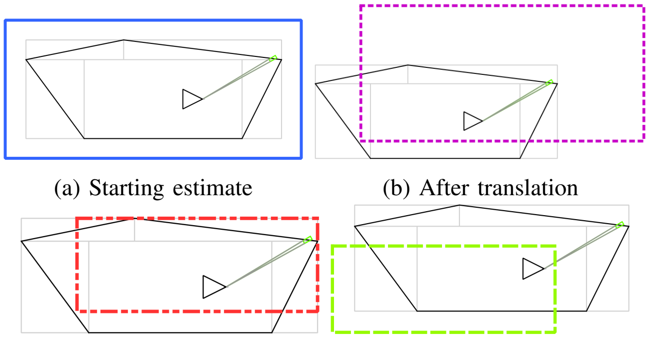

(a) Starting estimate (b) After translation

(c) After contraction around the walls (d) Final result after the inverse translation

Fig. 4: Localization process for a single measurement.

obstacles. In Line 6, the position box is translated along the measurement. Then, in Lines 7 to 10, the intersections between the translated position and each known wall is stored in $[\mathbf{p}_w]$, corresponding to the mixed pattern red line in Figure 4. If there was no wall and the result is still empty, then Line 12 is applied and $[\mathbf{p}_i]$ takes the value of the starting box, effectively ignoring the measurement. Otherwise, $[\mathbf{p}_w]$ is re-translated in the opposite direction and the result is stored in $[\mathbf{p}_i]$, in Line 14. Finally, $\mathbf{p}$ is contracted as the q-intersection of the $[\mathbf{p}_i]$. This process is coupled with the RSIVIA algorithm, which stops after the volume of the starting boxes reach an arbitrary minimum. In practice, the operations on intervals are computed

Procedure 1 Localization process

1: $[\mathbf{p}] = [\mathbf{D}]$
2: **for all** $([d_i], [\alpha_i])_{1 \le i \le n}$ **do**
3:     **if** $[d_i] \cap [0, \overline{d}] = \varnothing$ **then**
4:         $[d_i] = [\overline{d} - \Delta d/2, +\infty[$
5:     **end if**
6:     $[\mathbf{p}_t] = [\mathbf{p}] + [d_i] * \begin{pmatrix} [\cos]([\theta] + [\alpha_i]) \\ [\sin]([\theta] + [\alpha_i]) \end{pmatrix}$
7:     $[\mathbf{p}_w] = \varnothing$
8:     **for all** $([\mathbf{w}_k])_{1 \le k \le m}$ **do**
9:         $[\mathbf{p}_w] = [\mathbf{p}_w] \sqcup ([\mathbf{p}_t] \cap [\mathbf{w}_k])$
10:     **end for**
11:     **if** $[\mathbf{p}_w] = \varnothing$ **then**
12:         $[\mathbf{p}_i] = [\mathbf{p}]$
13:     **else**
14:         $[\mathbf{p}_i] = [\mathbf{p}_w] - [d_i] * \begin{pmatrix} [\cos]([\theta] + [\alpha_i]) \\ [\sin]([\theta] + [\alpha_i]) \end{pmatrix}$
15:     **end if**
16: **end for**
17: $[\mathbf{p}] = [\mathbf{p}] \bigcap_{i \in [\![1,n]\!]}^{\{q\}} [\mathbf{p}_i]$

using the Codac library [13]. This library provides standard contractors, operations, and inclusion functions for both real numbers and intervals, ensuring the enclosure of all solutions.

C. Computing the observation set

Now that the localization algorithm is defined, the last step is to use the estimability as defined earlier and provide an estimability map. Its goal is to illustrate, for each position on the map, if the algorithm can provide a good result. To generate this map, the starting domain $[\mathbf{D}]$ was divided into a grid G. For each cell $[\mathbf{p}] \in G$, the corresponding observations $[\mathbf{f}_i]([\mathbf{p}], [\mathbf{w}]) = ([d_i], [\alpha_i])^T$ are computed using the knowledge on the environment. The i-th ray intersects a segment defined by the points $\mathbf{a}$ and $\mathbf{b}$ if the position $\mathbf{p}$ and heading θ satisfy:

$$\det(\mathbf{a} - \mathbf{p}, (\begin{smallmatrix} \cos(\theta+\alpha_i) \\ \sin(\theta+\alpha_i) \end{smallmatrix})) \cdot \det(\mathbf{b} - \mathbf{p}, (\begin{smallmatrix} \cos(\theta+\alpha_i) \\ \sin(\theta+\alpha_i) \end{smallmatrix})) \le 0 \quad (16)$$

Then, the distance from the system's position to the considered segment is given by:

$$d_i = \frac{\det(\mathbf{a} - \mathbf{p}, \mathbf{b} - \mathbf{a})}{\det((\begin{smallmatrix} \cos(\theta+\alpha_i) \\ \sin(\theta+\alpha_i) \end{smallmatrix}), \mathbf{b} - \mathbf{a})} \quad (17)$$

If $d_i \notin [0, \overline{d}]$, then the wall is considered as not detected. The constraints presented are applied to the interval representation of the different variables involved. Since there are some ambiguous cases where a sensor beam can potentially cross several walls, the output is the union of possible distances. If no wall is detected, then the returned distance interval is $[\overline{d}, +\infty[$. Finally, the observation set $\mathbb{Y}_i(\mathbf{p})$ is computed. Since the error is centered, the set $\{\mathbf{e}_2 - \mathbf{e}_1 \mid (\mathbf{e}_1, \mathbf{e}_2) \in E_i^2\}$ becomes $2 \cdot E_i$, which means for our application:

$$\mathbb{Y}_i(\mathbf{p}) \subseteq [\mathbf{f}_i]([\mathbf{p}], [\mathbf{w}]) + ([-\Delta d, \Delta d], [-\Delta\alpha, \Delta\alpha])^T \quad (18)$$

D. First localization results

To ensure that the localization process is relevant, it was tested in the company common spaces. The room's walls were mapped using measuring tape. The boxes used to represent them are large enough to take into account measurements uncertainties. Other obstacles, like furniture, or the lower half of the staircase, were roughly positioned and represented through bigger boxes. See Figure 5 for the resulting map. The

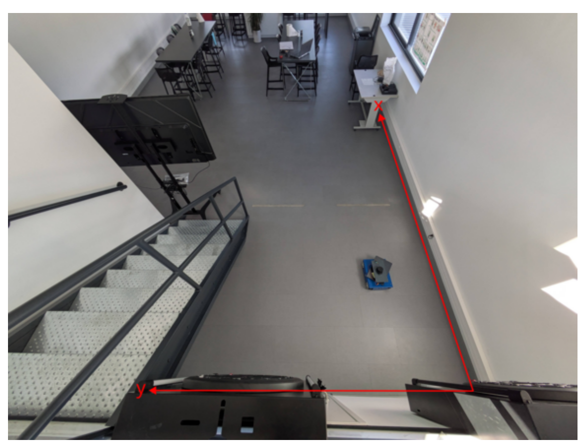

Fig. 5: The room used for the experiment.

sensor used is a LiDAR with the following parameters:

- Number of measurements $n = 252$;
- Maximum range $\bar{d} = 6$ m;
- Maximum error on the measured range $\Delta d < 0.5$ m;
- Maximum error on the ray orientation $\Delta\alpha < 1°$.
- Maximum number of outliers $q = 20$;

The outlier budget was inferred experimentally, and reflects the poorly made map, that does not account for every obstacle in the room. The localization algorithm was launched with these parameters and the starting domain $[\mathbf{D}] = [-0.05, 12.05] \times [-0.05, 6.77]$ meters. The results for two different starting poses are presented in Figure 6.

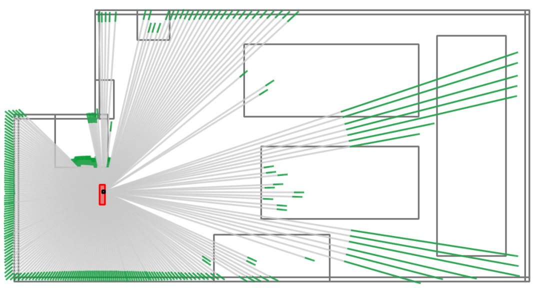

(a) Pose 1

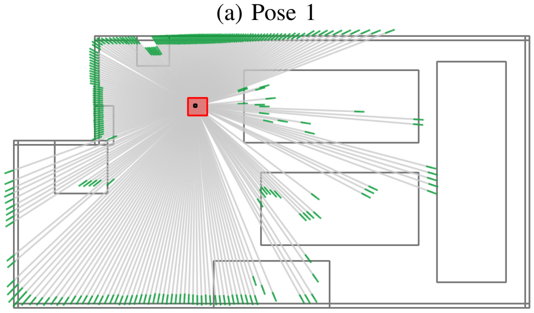

(b) Pose 2

Fig. 6: Localization results. The small black box is the measured position; the larger red box is the estimated result. The numerical value are detailed in the Table I.

TABLE I: Measured vs. estimated positions for the two test poses.

	Pose 1	Pose 2
Heading θ (°)	$[-5, 5]$	$[-40, -32]$
Measured (x, m)	$[1.99, 2.05]$	$[4.15, 4.21]$
Estimated (x, m)	$[1.96, 2.08]$	$[4.03, 4.49]$
Measured (y, m)	$[2.00, 2.06]$	$[4.63, 4.69]$
Estimated (y, m)	$[1.76, 2.22]$	$[4.46, 4.87]$

E. Generating the estimability map

Since we lacked a precise cartography for the environment at hand, introducing outliers and generating an estimability map is done for a simulated environment illustrated in Figure 7, with the parameters:

- Number of measurements $n = 36$;
- Space between measurements $\alpha_{i+1} - \alpha_i = 1°$;
- Maximum range $\bar{d} = 7$ m;
- Maximum error on the measured range $\Delta d < 0.5$ m;
- Maximum error on the ray orientation $\Delta\alpha < 2°$.

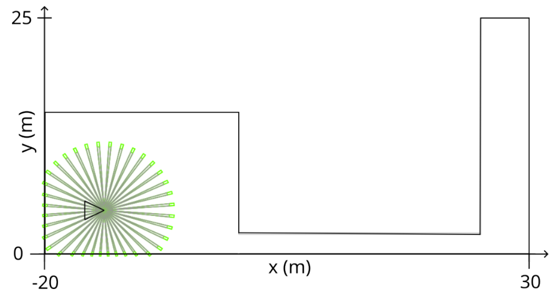

Fig. 7: Map and sensors parameters used in the simulation.

As briefly mentioned in Section II.F, there are different ways to quantify the estimability of the position $\mathbf{p}$ using $\hat{\mathbb{P}}$. The set-inversion algorithm outputs a list of solution containing interval vectors, of which we take the union. Two functions were tested:

1) The surface of the output;
2) The width of each dimension of the output.

The starting domain $\mathbf{D}$ was divided in cells of 1×1 meter. An estimability map was generated for a few values of q. In

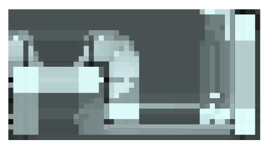

(a) $q = 0$

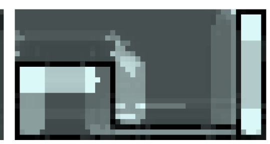

(b) $q = 2$

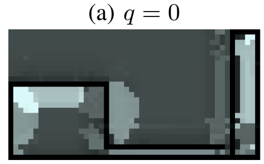

(c) $q = 5$

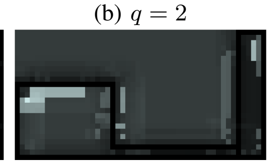

(d) $q = 8$

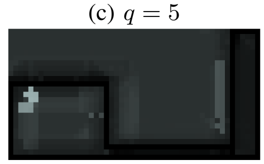

(e) $q = 10$

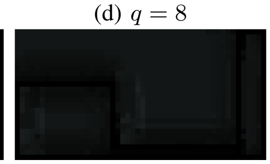

(f) $q = 15$

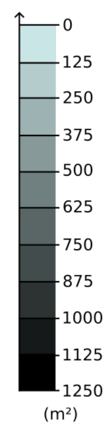

Fig. 8: Resulting estimability maps for growing values of MNO, using the surface of the result in square meters. Corresponding legend on the left, with 1250 m^2 being the size of $\mathbf{D}$.

Figure 8, we can see exactly how and where the localization is worsened as the hypothesis on outliers becomes more pessimistic. The corners of the environment are the most robust locations, while empty space and corridors degrade faster, since they translate lesser information. Looking at the result in Figure 9 with $q \in \{0, 5\}$, as expected, knowledge on the x coordinate is better in the vertical corridor, and knowledge on the y coordinate is better in the horizontal corridor. Although, with $q = 10$, performances degrade altogether.

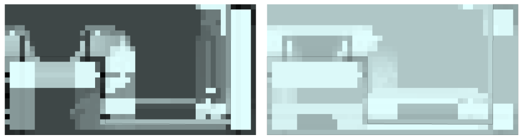

(a) $q = 0$

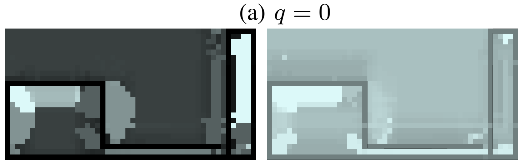

(b) $q = 5$

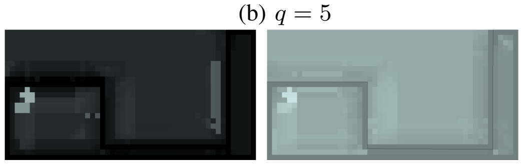

(c) $q = 10$

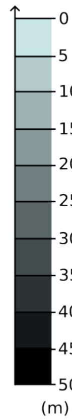

Fig. 9: Resulting estimability maps for growing values of MNO, with the width along the x-axis on the left column, and the width along the y-axis on the right.

IV. Discussions

A. On the identification of sensor failure

In some cases, outliers in measurements can be caused by a sensor complete failure. With multiple telemeters, in a dynamic context, if the system can diagnose that a sensor is consistently giving outliers measurements, a strategy to explore would be to ignore this sensor for the next iterations of the localization process.

In a similar manner, knowledge on environmental parameters could be updated if they are found consistently incompatible with the measurements. This can happen in a localization context if a wall is found to be consistently undetected or inconsistent with the measurements.

B. On other estimability functions

Beyond the surface area metric chosen in this work, several alternative estimability functions merit investigation:

- **Obstacle avoidance capacity:** Estimating the minimum distance to detected obstacles relative to the localization uncertainty could be used when validating safety margins for path planning;
- **Distance to a reference trajectory:** A predetermined path can be a better and more relevant reference than the reference frame axes, which were used in this work. Especially in environments with a more complex geometry, not necessarily aligned with said axes.

A comparison with an adaptation of stochastic methods such as [4] would allow for a relevant performance comparison.

V. Conclusion

This article has presented a general robust guaranteed estimability computation and mapping, using Interval Analysis. While previous definitions only took into account the presence of a bounded noise, this method works with a maximum number of outliers assumption and external environmental parameters in the constraints equations. We illustrated this method for the localization of a vehicle equipped with telemeters. The estimability maps generated can be used to perform mission planning and risk assessment, and more rigorous localization performances analysis, for example in the PANORAMA method [14].

Among perspectives, the next step would be the integration of an evolution function to apply the method to dynamic systems [12], paired with computation optimization in rays intersections and searches, as well as sensor failure identification as discussed. We could also better the characterization of measurements with potential outliers using the tools of [15].

References

[1] S. Thrun, W. Burgard, and D. Fox, *Probabilistic Robotics*. Cambridge: The MIT Press, 2005. [Online]. Available: https://mitpress.mit.edu/9780262201629/probabilistic-robotics/

[2] E. Walther, S. Khattak, and M. Hutter, *Learning-based Localizability Estimation for Robust LiDAR Localization*, Oct. 2022.

[3] N. Roy, W. Burgard, D. Fox, and S. Thrun, *Coastal navigation-mobile robot navigation with uncertainty in dynamic environments*, Feb. 1999, vol. 1, journal Abbreviation: Proceedings - IEEE International Conference on Robotics and Automation Pages: 40 vol.1 Publication Title: Proceedings - IEEE International Conference on Robotics and Automation.

[4] W. Zhen, S. Zeng, and S. Soberer, “Robust localization and localizability estimation with a rotating laser scanner,” in *2017 IEEE International Conference on Robotics and Automation (ICRA)*, May 2017, pp. 6240–6245. [Online]. Available: https://ieeexplore.ieee.org/document/7989739/

[5] R. E. Moore, *Methods and Applications of Interval Analysis*. Philadelphia, PA: SIAM, 1979.

[6] O. Reynet and L. Jaulin, “A new interval-based method to characterize estimability,” *International Journal of Adaptative Control and Signal Processing*, vol. 25, no. 3, pp. 288–294, 2011.

[7] L. Jaulin, M. Kieffer, O. Didrit, and E. Walter, *Applied Interval Analysis*. Springer, 2001.

[8] M. Mustafa, A. Stancu, N. Delanoue, and E. Codres, “Guaranteed SLAM—An interval approach,” *Robotics and Autonomous Systems*, vol. 100, pp. 160–170, 2018. [Online]. Available: https://www.sciencedirect.com/science/article/pii/S0921889017303986

[9] R. Guyonneau, S. Lagrange, and L. Hardouin, “A visibility information for multi-robot localization,” in *IEEE/RSJ International Conference on Intelligent Robots and Systems (IROS)*, 2013.

[10] B. Telle, M.-J. Aldon, and N. Ramdani, “Guaranteed 3D visual sensing based on interval analysis,” in *Proceedings 2003 IEEE/RSJ International Conference on Intelligent Robots and Systems (IROS 2003) (Cat. No.03CH37453)*, vol. 2, 2003, pp. 1566–1571 vol.2.

[11] B. Desrochers, S. Lacroix, and L. Jaulin, “Set-membership approach to the kidnapped robot problem,” in *IROS 2015*, 2015.

[12] L. Jaulin, “Robust set-membership state estimation; application to underwater robotics,” *Automatica*, vol. 45, no. 1, pp. 202–206, 2009.

[13] S. Rohou, B. Desrochers, and F. L. Bars, “The Codac Library: A Catalog of Domains and Contractors,” *Acta Cybernetica*, vol. 26, no. 4, pp. 871–887, Mar. 2024. [Online]. Available: https://cyber.bibl.u-szeged.hu/index.php/actcybern/article/view/4388

[14] P. Lambert, “Contribution à l’autonomie des robots : vers des missions à garantie de performance incluant l’incertitude de localisation en environnement intérieur connu,” Theses, Université Montpellier, Jun. 2021, issue: 2021MONTS018. [Online]. Available: https://theses.hal.science/tel-03384111

[15] J. Tillet, L. Jaulin, F. Le Bars, and R. Boukezzoula, “A fuzzy set estimation using interval contractors: Application to localization,” *Reliable Computing*, vol. 29, pp. 4–25, 2022.